



HAL
open science

A FINITE VOLUME SCHEME FOR THE SHALLOW-WATER SYSTEM WITH THE POLYNOMIAL RECONSTRUCTION

Stéphane Clain, Jorge Figueiredo, Carolina Ribeiro

► **To cite this version:**

Stéphane Clain, Jorge Figueiredo, Carolina Ribeiro. A FINITE VOLUME SCHEME FOR THE SHALLOW-WATER SYSTEM WITH THE POLYNOMIAL RECONSTRUCTION. 2012. hal-00675745

HAL Id: hal-00675745

<https://hal.science/hal-00675745>

Preprint submitted on 1 Mar 2012

HAL is a multi-disciplinary open access archive for the deposit and dissemination of scientific research documents, whether they are published or not. The documents may come from teaching and research institutions in France or abroad, or from public or private research centers.

L'archive ouverte pluridisciplinaire **HAL**, est destinée au dépôt et à la diffusion de documents scientifiques de niveau recherche, publiés ou non, émanant des établissements d'enseignement et de recherche français ou étrangers, des laboratoires publics ou privés.

A FINITE VOLUME SCHEME FOR THE SHALLOW-WATER SYSTEM WITH THE POLYNOMIAL RECONSTRUCTION

Clain, S., Figueiredo, J., Ribeiro, C.

*Departamento de Matemática e Aplicações e Centro de Matemática,
Universidade do Minho, Campus de Azurém, 4800-058 Guimarães,
jmfiguei@math.uminho.pt*

INTRODUCTION

We present a new very high-order finite volume scheme for the shallow-water system based on the local Polynomial Reconstruction Operator (PRO-scheme) and the MOOD technique to guaranty the solution stability. We detail the design of the scheme and provide two examples with regular solution of wave propagation to highlight the scheme capacity to preserve the waves.

Keywords: SHALLOW-WATER, FINITE VOLUME, POLYNOMIAL RECONSTRUCTION.

1. THE SHALLOW-WATER PROBLEM

The Shallow-water system is very popular to model river or ocean flow for engineering or environmental purposes. Producing very efficient numerical schemes to obtain accurate and relevant approximations is a constant challenging objective. We here propose a new approach based on two ingredients: a finite volume scheme coupled with the Polynomial Reconstruction Operator (PRO-scheme) to achieve a very high-order algorithm. We consider the shallow-water problem $\partial_t U + \nabla \cdot \mathbf{F}(U) = S$, with U the conservative variables, $F(U) = (F_x(U), F_y(U))$ the flux vector, and S the source term given by

$$U = \begin{pmatrix} h \\ hu \\ hv \end{pmatrix}, \quad F_x(U) = \begin{pmatrix} hu \\ hu^2 + gh^2 \\ huv \end{pmatrix}, \quad F_y(U) = \begin{pmatrix} hu \\ huv \\ hv^2 + gh^2 \end{pmatrix}, \quad S(U) = \begin{pmatrix} 0 \\ -gh\partial_x z \\ -gh\partial_y z \end{pmatrix},$$

where h, u, v are, respectively, the water height and the two velocity components, and $z = z(x, y)$ is the bathymetry of the soil with respect to a reference altitude. In the present study we assume a regular bathymetry function such that its derivatives are regular enough.

2. A NEW FINITE VOLUME SCHEME

We consider a mesh T_h of triangle polyhedral cells K_i and edges $e_{ij} = K_i \cap K_j$, where n_{ij} are the outward normal vectors, $j \in \nu(i)$ the index set of the neighbor cells of K_i . For each e_{ij} , q_{ij}^r are the associated Gauss points on the edge (see Figure 1).

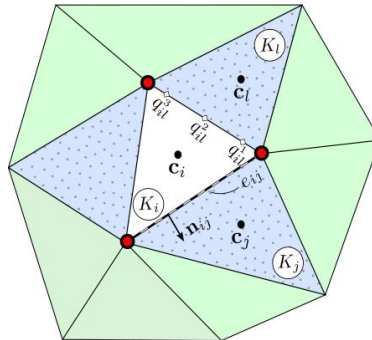


Figure 1 – Mesh notations.

Let us denote by U_i^n an approximation of the mean value of U over cell K_i at time t^n . To provide an approximation at time t^{n+1} , the generic very high-order finite volume scheme writes:

$$U_i^{n+1} = U_i^n - \Delta t \sum_{j \in \nu(i)} \sum_{r=1,2,3} \omega_r \frac{|e_{ij}|}{|K_i|} \mathcal{F}(U_{ij,r}^n, U_{ji,r}^n, n_{ij}) + S_i^n,$$

with ω_r the associated weights for the integration quadrature rule over the edge, $|e_{ij}|$ and $|K_i|$ are the length and area respectively. Function $\mathcal{F}(U_{ij,r}^n, U_{ji,r}^n, n_{ij})$ is the numerical flux evaluated at the Gauss points (for instance a Rusanov or HLL flux as presented in LeVeque book) and S_i^n the source term. The point is the calculation of the approximation at the Gauss points.

To this end, for a given piecewise constant function $(q_i)_{K_i \in \mathcal{T}_h}$, we introduce the polynomial function of degree d with $\alpha = (\alpha_1, \alpha_2)$ the multi-index and $|\alpha| = \alpha_1 + \alpha_2$:

$$\hat{q}_i(x, y) = q_i + \sum_{1 \leq |\alpha| \leq d} \mathfrak{R}_\alpha \{ (x - c_x)^{\alpha_1} (y - c_y)^{\alpha_2} - M_\alpha \}, \quad M_\alpha = \frac{1}{|K_i|} \int_{K_i} (x - c_x)^{\alpha_1} (y - c_y)^{\alpha_2} dx dy,$$

where we determine the coefficients $\mathfrak{R} = (\mathfrak{R}_\alpha)$ minimizing the functional

$$E(\mathfrak{R}) = \sum_{c_j \in \text{stencil}} \left[q_j - \frac{1}{|K_i|} \int_{K_i} \hat{q}_i(x, y) dx dy \right]^2.$$

To achieve a solution, one has to provide a rich enough stencil, *i.e.* a set of cells around K_i . We compute the polynomial approximation on each cell for variables $q = h, uh, vh$ and z and we set $q_{ij,r} = \hat{q}_i(\mathbf{g}_{ij,r})$, while the source term writes

$$S_i^n = - \frac{1}{|K_i|} \int_{K_i} g \hat{h}_i \begin{pmatrix} 0 \\ \partial_x \\ \partial_y \end{pmatrix} \hat{z}_i dx dy.$$

3. THE MOOD PROCEDURE

It is well-known that numerical solutions for the shallow water problem may present discontinuities, hence a very high-order scheme in the vicinity of such discontinuities does not make sense and one has to recover the former first-order finite volume scheme to provide stability. To this end, we employ the Multi-dimensional Optimal Order Detection procedure (MOOD) to detect the cells where the high-order reconstruction is not eligible. We briefly recall the principle of the method (see Clain et al. 2011). The technique is based on a *a posteriori* detection procedure for the eligibility of the solution.

Assume that we have a numerical solution $U^n = (U_i^n)$ for time t^n , we mark each cell K_i with the current polynomial degree d_i and initialize to the maximum degree d_{max} of the method. We then compute the polynomial reconstruction $\hat{q}_i^n(x, y)$ of degree d_i for the three variables $q = h, uh, vh$ at time t^n , determine the flux approximation at the Gauss points and at finally we evaluate a candidate solution $U^* = (U_i^*)$ at time t^{n+1} .

At that point we determine whether the solution is eligible. We introduce the following detector procedure: the solution $h_i^*, (uh)_i^*, (vh)_i^*$ is eligible if

- the solution is physically admissible, *i.e.* $h_i^* \geq 0$;
- we have a local maximum principle for the height function

$$\min_{j \in \nu(i)} (h_i^n, h_j^n) \leq h_i^* \leq \max_{j \in \nu(i)} (h_i^n, h_j^n).$$

If the solution on cell K_i is not eligible, then we decrement the polynomial degree of the reconstruction setting $d_i := d_i - 1$. Note that for $d_i = 0$ the solution will satisfy the two criteria above since we employ a positive preserving flux which respects the maximum principle for the height. When all the cells are considered eligible, we set $U^{n+1} = U^*$ as the solution at time t^{n+1} . Other more sophisticated detection procedure can be found in Clain et al. (2012).

4. NUMERICAL SIMULATIONS

To show the performance of the numerical scheme described in the previous section we carried out three numerical simulations that we shall refer to as Test 1, Test 2 and Test 3, all of them using reflection boundary conditions and a mesh of triangles. The Rusanov flux scheme is used in all simulations and, when applicable, the polynomial reconstruction for z is P2. For sake of simplicity, we define $H(x, y) = h(x, y) + z(x, y)$ as the water height with respect to a reference altitude. We will also denote by $\|\cdot\|$ the standard L^∞ norm.

Test 1: Basin test

The goal of the present test is to check that the steady-state situation (the lake at rest) is preserved. To this we have carried out the simulation during the effective time $t = 0.1$.

Figure 2 presents the geometry considered for the basin: $[0, 1] \times [0, 0.5]$. The initial water level H is equal to 1 and the system is at rest, i.e. $V = (u, v) = 0$, and $z = x(0.75 + 2(y - 0.25)^2)$.

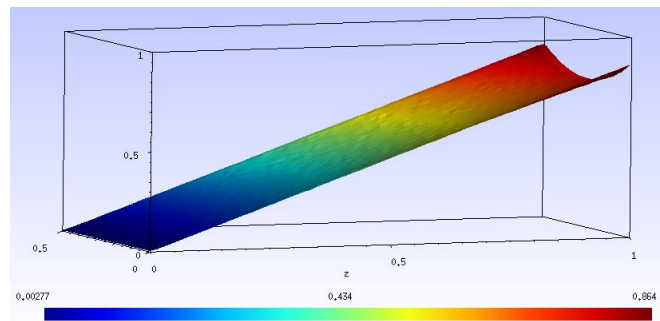


Figure 2 – Test 1 geometry.

Given the initial conditions, we expect that both h and V remain equal to zero along the simulation. Figure 3 illustrates the results obtained at $t = 0.1$ when P0 and P3 polynomials are used for the reconstruction of U .

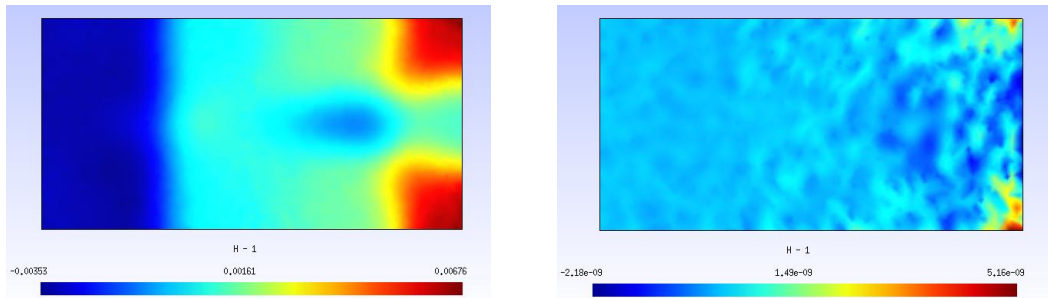


Figure 3a – Representation of $H - 1$ for P0 (left) and P3 (right) approximations at $t = 0.1$.

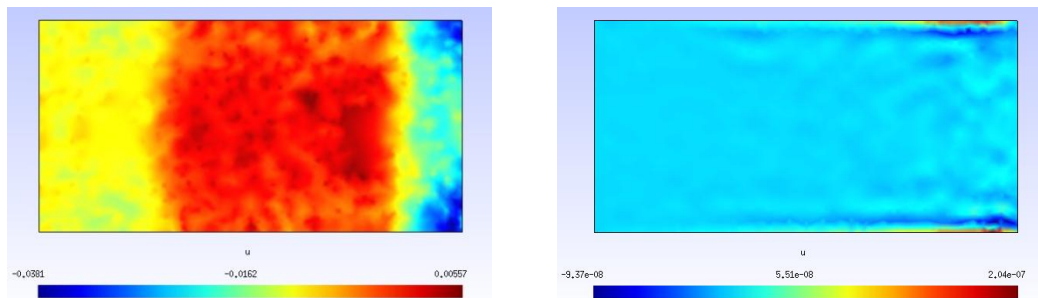


Figure 3b – Representation of u for P0 (left) and P3 (right) approximations at $t = 0.1$.

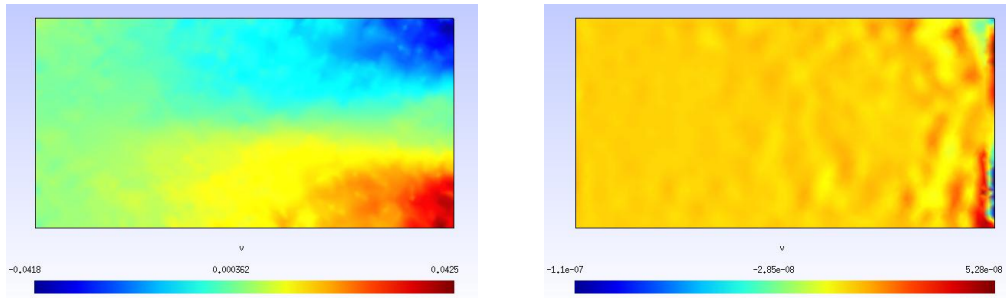


Figure 3c – Representation of v for P0 (left) and P3 (right) approximations at $t = 0.1$.

The results clearly show a considerable improvement when the polynomial degree is increased and agree with the expected result (steady-state solution). In fact, one has $\|H - 1\| \sim 10^{-2}, 10^{-4}, 10^{-5}, 10^{-8}$ and $\|V\| \sim 10^{-1}, 10^{-3}, 10^{-4}, 10^{-7}$ when P0, P1, P2 and P3 polynomials, respectively, are used for the reconstruction.

Test 2: Tsunami propagation (flat soil)

In the second test we aim to simulate the wave propagation with a strong initial perturbation of the lake at rest (around 10% of the initial height).

Figure 4 presents the geometry used in this test: $[0, 5] \times [0, 0.5]$. The initial water level is now given by the analytical relation: $H = 1 + 0.1 \exp(-500(x - 2.5)^2)$, while we set $V = 0$ and $z = 0$.

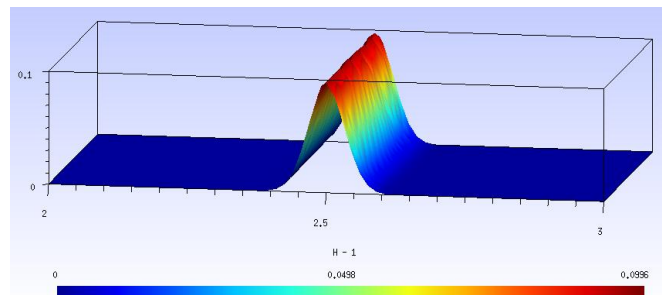


Figure 4 – Test 2 geometry (cut) and initial H profile.

As in the previous test, we simulated the evolution of the system using P0, P1, P2 and P3 polynomials. Given the symmetry of the problem, the initial wave evolve into two waves that are symmetric with respect to $x = 2.5$. Figure 5 illustrates the results obtained for H at $t = 0.65$.

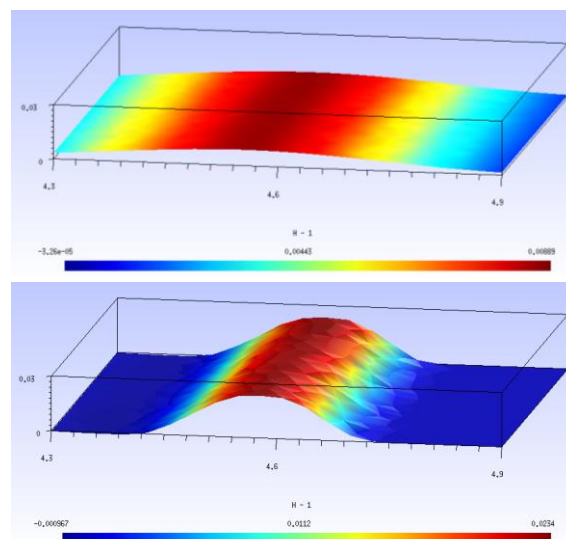


Figure 5a – Representation of $H - 1$ for P0 (left) and P1 (right) approximations at $t = 0.65$.

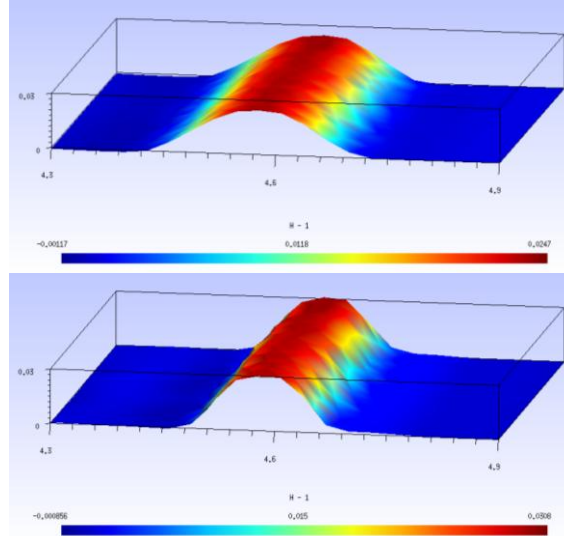


Figure 5b – Representation of $H - 1$ for P2 (left) and P3 (right) approximations at $t = 0.65$.

As expected, numerical diffusion “destroys” the wave when P0 polynomials are used and both the wave height and shape are progressively recovered as the polynomial degree used increases. In fact, at $t = 0.65$ we obtain: $\|H - 1\| = 0.009, 0.023, 0.025, 0.031$ for P0 to P3, respectively. Another important aspect has to do with the use of MOOD procedure, which prevents the appearance of artificial oscillations in the solution even when P3 polynomials are used. Figure 6 represents the results obtained for $t = 0.65$ using a P1 approximation if MOOD is not used. The oscillations with respect to the reference level $H = 1$ are clearly present.

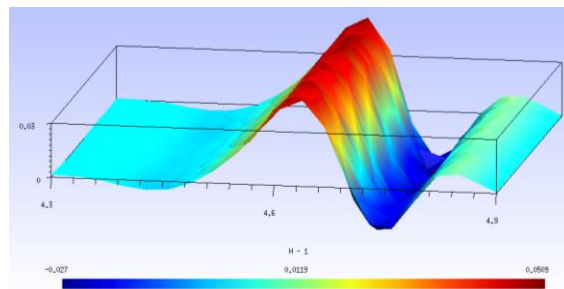


Figure 6 – Representation of $H - 1$ at $t = 0.65$ using a P1 approximation with no MOOD procedure.

Test 3: Tsunami propagation (non-flat soil)

The last test concerns the wave propagation on a non-flat soil.

In this simulation the geometry is the same used in Test 1, but now $H = 1 + 0.2 \exp(-20(x - 2.5)^2)$. The bathymetry of the soil is the same as in Test 1, but scaled to account for the difference in the domain span along the x -direction, i.e. $z = 0.2x(0.75 + 2(y - 0.25)^2)$. Figure 7 presents the initial situation of the system as far as H and z are concerned.

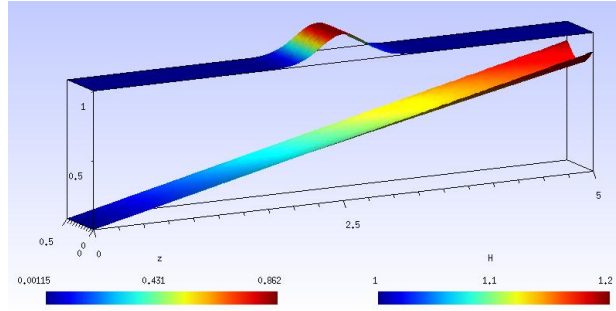


Figure 7 – Test 3 geometry and initial H profile.

We simulated the evolution of the two waves that originate from the initial perturbation up to $t = 0.6$. The results obtained using P0, P1 and P3 polynomials for the reconstruction are presented in Figure 8 (the P2 case is very similar to the P1 one and is therefore omitted).

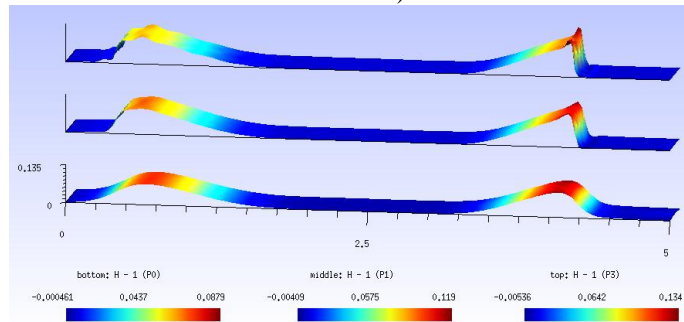


Figure 8 – Representation of $H - 1$ for $t = 0.6$ using P0 (bottom), P1 and P3 (top) polynomials.

Given the bathymetry of the soil, the left wave is expected to travel faster than the right one. That can be observed in the simulations independently of the degree of polynomials used. However, as seen in Test 2, the numerical diffusion of the lowest order scheme leads to a considerable loss in the amplitude of the travelling waves and is not able to reproduce the wave profile correctly (shock almost absent). On the contrary, higher order schemes are able to capture the shock in a much clearer way without presenting artificial oscillations (especially in the P1 and P2 cases). As far as H is concerned, we obtained $\|H - 1\| = 0.088, 0.119, 0.121, 0.134$ for the P0 to P3 cases, respectively.

5. CONCLUSIONS

Numerical simulations were carried out to highlight the performance of the numerical scheme to reduce the numerical viscosity and provide very accurate solutions. For instance, the scheme manages to handle travelling waves during very long times like tsunamis. We also verified that the scheme preserves the steady-state solution, namely lake at rest. The coupling of the PRO-scheme with the MOOD technique produces very good approximations. Nevertheless, two important tasks remain: a more efficient detecting procedure for the MOOD contribution and a wet/dry algorithm to take into account the emerged part of the domain.

6. REFERENCES

- S. Clain, S. Diot, R. Loubère, A high-order polynomial finite volume method for hyperbolic system of conservation laws with Multi-dimensional Optimal Order Detection (MOOD), Journal of computational Physics, Volume 230, 4028-4050, 2011.
- S. Clain, D. Rochette, First and Second order finite volume methods for non-conservative Euler system, Journal of computational Physics, 228 (2009) 8214-8248.
- S. Clain, S. Diot, R. Loubère, submitted in, Computers & Fluids, under corrections (2012).

D. Rochette, S. Clain, W. Bussi re, Unsteady compressible flow in ducts with varying cross-section: comparison between the non-conservative Euler system and the axisymmetric flow model, *Computers & Fluids* 53 (2012) 53-78.

R. J. LeVeque, *Finite Volume Methods for Hyperbolic Problems*, Cambridge University Press, 2002.